Inorganica Chimica Acta 518 (2021) 120245

Contents lists available at ScienceDirect

Inorganica Chimica Acta

journal homepage: www.elsevier.com/locate/ica

Research paper

Hydrogen and chemicals from alcohols through electrochemical reforming by Pd-CeO_2/C electrocatalyst

Marco Bellini [a], Maria V. Pagliaro [a], Andrea Marchionni [a], Jonathan Filippi [a], Hamish A. Miller [a,*], Manuela Bevilacqua [a], Alessandro Lavacchi [a], Werner Oberhauser [a], Jafar Mahmoudian [a], Massimo Innocenti [a,c], Paolo Fornasiero [a,b,*], Francesco Vizza [a,*]

[a] Istituto di Chimica dei Composti Organometallici (CNR-ICCOM), Via Madonna del Piano 10, 50019, Sesto Fiorentino, Italy
[b] Department of Chemical and Pharmaceutical Sciences, University of Trieste, Via L. Giorgieri 1, 34127, Trieste, Italy
[c] Dipartimento di Chimica 'Ugo Schiff', Università degli Studi Firenze, Via della Lastruccia, 3-13, 50019 Sesto Fiorentino, Italy

ARTICLE INFO

Keywords:
Electrocatalysis
Hydrogen
Alcohol electroreforming
Renewable feedstock
Valuable chemicals

ABSTRACT

The development of low-cost and sustainable hydrogen production is of primary importance for a future transition to sustainable energy. In this work, the selective and simultaneous production of pure hydrogen and chemicals from renewable alcohols is achieved using an anion exchange membrane electrolysis cell (electrochemical reforming) employing a nanostructured Pd-CeO_2/C anode. The catalyst exhibits high activity for alcohol electrooxidation (e.g. 474 mA cm^{-2} with EtOH at 60 °C) and the electrolysis cell produces high volumes of hydrogen (1.73 l min^{-1} m^{-2}) at low electrical energy input (E_{cost} = 6 kWh $kg_{H_2}{}^{-1}$ with formate as substrate). A complete analysis of the alcohol oxidation products from several alcohols (methanol, ethanol, 1,2-propandiol, ethylene glycol, glycerol and 1,4-butanediol) shows high selectivity in the formation of valuable chemicals such as acetate from ethanol (100%) and lactate from 1,2-propandiol (84%). Importantly for industrial application, in batch experiments the Pd-CeO_2/C catalyst achieves conversion efficiencies above 80% for both formate and methanol, and 95% for ethanol.

1. Introduction

Modern human society is reliant on fossil fuels. Since the oil crises of the early 1970s it has become clear this system is not sustainable. This has led to a huge effort to find alternative energy resources based on renewables [1–3]. Molecular hydrogen has a key role as high-quality energy carrier for replacing fossil fuels [4]. Despite intensive research, hydrogen as energy carrier has not yet reached worldwide utilization due to several issues. Firstly, no market scale technology has been developed yet for H_2 production, storage and conversion to electricity matching the necessary sustainable and low-cost criteria [5–9]. A well-known and consolidate process for hydrogen production is the electrolysis of water; it is the only route able to convert renewable energy sources (e.g., photovoltaic, wind, biomass, geothermal) into 99.999% pure hydrogen [10,11]. Polymer Exchange Membrane Electrolysers (PEM-Electrolysers) are the most performing devices ever reported, nevertheless they don't have a significant commercial impact owing to high operative costs [5]. The best PEM electrolysers still require high electric energy input, up to 50 kWh $kg_{H_2}{}^{-1}$, indeed they need precious metal based catalyst at high loadings and an expensive polymer exchange membrane [12]. The anodic Oxygen Evolution Reaction (OER) contributes mostly to the high PEM-electrolyser energy input. Replacing it with the more efficient oxidation of a sacrificial molecule, e.g. an alcohol [13–15] or ammonia [16,17], is a strategy to lower the high electrolysis energy cost. "Electrochemical Reforming" or "electroreforming" matches the anodic oxidation of aliphatic alcohols with the cathodic water reduction to hydrogen and the resulting electrolysis process occurs at cell potentials lower than 1 V, dropping the energy input to c.a. 20 kWh $kg_{H_2}{}^{-1}$ [18–21]. A scheme of anion exchange membrane based electroreforming is reported in Fig. 1. The strong alkaline environment (pH greater than 12) allows the partial oxidation of alcohols to valuable chemicals, such as carboxylic compounds, which are raw materials for fine chemicals industry. So alcohol electroreformers are the only electrochemical devices able to store electric energy in molecular hydrogen and convert a biomass derived alcohol into high added value chemicals [19]. In addition, alcohol oxidation reactions

* Corresponding authors.
E-mail addresses: hamish.miller@iccom.cnr.it (H.A. Miller), pfornasiero@units.it (P. Fornasiero), francesco.vizza@iccom.cnr.it (F. Vizza).

https://doi.org/10.1016/j.ica.2021.120245
Received 2 December 2020; Received in revised form 30 December 2020; Accepted 30 December 2020
Available online 12 January 2021

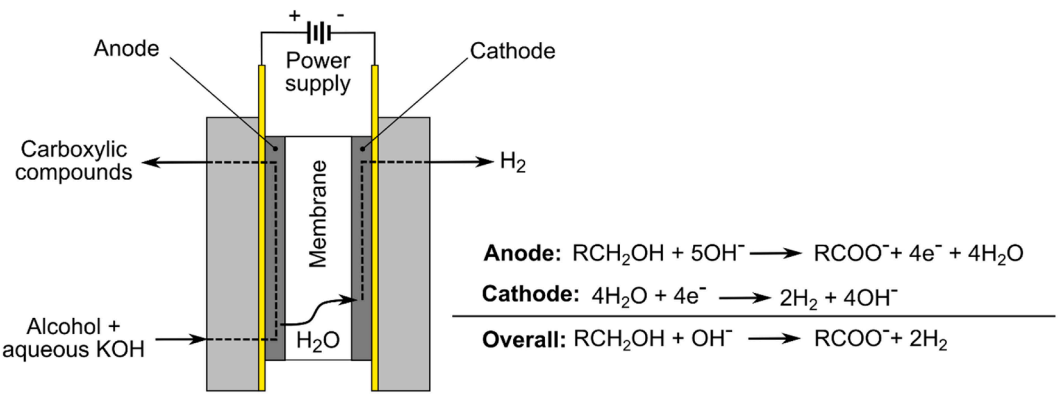

Fig. 1. A simplified scheme of a state of the art alkaline electroreforming cell.

have faster kinetics in alkaline media, improving the electroreformer efficiency [22]. Several renewable source derived alcohols have been investigated as fuel for alkaline electroreforming cells, such as methanol, ethanol, 1,2-propandiol, ethylene glycol, glycerol, 1,4-butanediol [23–26]. Formate is an attractive sacrificial molecule as well, since it is a derivative of formic acid, which can be produced from renewable sources such as the electrochemical reduction or catalytic hydrogenation of CO_2. To make formic acid (and formate) a sustainable fuel, the electric energy or hydrogen employed in such processes must be derived from neutral sources [27]. Formate salts are more appealing than volatile formic acid solutions because as solids they can be easily stored, transported and safely handled and fuels can be obtained just mixing the salts with water [28].

Palladium nanoparticles supported on carbon black (Pd/C) and their derivatives represent the state of the art anodic catalysts for alcohols and formate oxidation in alkaline electroreforming [29,30]. In previous papers [31,32] we have investigated palladium nanoparticles on a ceria decorated carbon black support (50% wt C and 50% wt CeO_2) obtaining a high efficiency anode, Pd-CeO_2/C, for low aliphatic alcohols and formate oxidation in alkaline direct fuel cells. Cerium (IV) oxide is a cheap and not toxic material with a relative high natural availability. Moreover, CeO_2 redox properties makes this material suitable for several catalytic applications, spanning from electrocatalysis (e.g. fuel cells, water electrolysis and CO_2 reduction to fuels) to homogeneous catalysis (e.g for water gas shift reaction) [33–35]. Unfortunately, ceria is a semiconductive material, so for electrocatalytic applications it is often combined with a conductive support, such as carbon based materials (carbon black, carbon nanotubes or graphene) [33]. CeO_2 can easily change the oxidation state switching between Ce^{3+} and Ce^{4+} and acting as an oxygen buffer in the catalytic material. In particular, in palladium-ceria electrocatalysts for alcohol oxidation, CeO_2 promotes the OH^- ions spillover to the metal nanoparticles [35]. So in the Pd-CeO_2/C catalyst, Pd(I)-OH_{ads} formation happens at lower potentials compared to Pd/C analogue catalysts, enhancing the electrocatalytic activity [36]. In a similar manner, ceria enhances Pd activity in formate electrooxidation [27]. Most of the technology developed for direct alcohol and formate fuel cells can be transferred to electroreforming [15]. In this article, the Pd-CeO_2/C anode is assembled in a complete electroreformer, together with a commercial AEM membrane (Tokuyama A201) and a commercial Pt/C cathode. The cell was fed with formate and several alcohols, (methanol, ethanol, ethylene glycol, 1,2-propandiol, 1,4-butanediol and glycerol), demonstrating the high versatility of Pd-CeO_2/C catalyst given that the availability of biomass derived alcohols is strongly dependent on seasonality and on geographic areas of production [37]. The electroreformer reported here is able to produce a number of important chemicals including acetate, lactate, succinate and glycolate.

2. Experimental

2.1. Materials and methods

2.1.1. Synthesis of Pd-CeO_2/C

The anode catalyst Pd-CeO_2/C was synthesized by using a two step method as described previously [38]. In brief, the C-CeO_2 support was prepared suspending 4 g of carbon black (Vulcan XC-72, Cabot corp.) in 250 ml of distilled water. 10.1 g of $Ce(NO_3)_3{\cdot}6H_2O$ were dissolved in the suspension and the resulting solution was stirred for 60 min and further homogenized by ultrasonic treatment (30 min, 59 Hz, 100 W). The pH was adjusted to 12 adding dropwise a 0.45 M KOH aqueous solution and subsequently the suspension was stirred for 2 h. The solid product was separated by filtration and washed several times with distilled water until neutral pH was obtained. The product was dried at 65 °C and then heated under air in a tube furnace at 250 °C for 2 h. The furnace was cooled down to room temperature under Ar atmosphere.

Palladium nanoparticles were so grown onto C-CeO_2 support. 4 g of C-CeO_2 were suspended in water (500 ml) by a vigorous magnetic stirring (30 min) and a subsequent ultrasonic treatment (20 min, 59 Hz, 100 W). Then a 60 ml aqueous solution of K_2PdCl_4 (1.38 g) was added dropwise (approximately 1 h) under vigorous stirring. Palladium salt was reduced by adding dropwise a 2.5 M KOH (8.4 ml) aqueous solution and 50 ml of ethanol (99.9%, Sigma-Aldrich-Merck); the resulting mixture was heated at 80 °C for 60 min. The so obtained Pd-CeO_2/C catalyst was filtered off, washed several times with distilled water to neutrality, and finally dried under vacuum at 65 °C. The yield of Pd-CeO_2/C was of 97%.

2.1.2. Electron microscopy

Transmission electron microscopy (TEM) was performed on a Philips CM12 microscope using an accelerating voltage of 100 kV. Samples were prepared by suspending the catalyst in isopropanol applying ultrasounds for 20 min (59 Hz, 100 W). The suspension was then dropped onto the carbon coated copper TEM grids and dried under air.

2.1.3. Membrane electrode assemblies

Membrane electrode assemblies (MEAs) were prepared using the Pd-CeO_2/C anode electrocatalyst, a commercial anion exchange membrane, and a carbon cloth cathode containing a commercial 40 wt% Pt/C catalyst (Aldrich). The anion exchange solid polymer membrane used is a Tokuyama A201 obtained from Tokuyama Corp. (Japan). Prior to use, membrane counter ions were exchanged with OH^- groups by soaking the membrane in 1 M KOH for 24 h. The membrane was then washed thoroughly in deionized water. The cathode electrode was prepared by spreading a catalyst ink onto a carbon cloth W1S1005 (CeTech Co., Ltd.) gas diffusion layer, with a Meyer rod (n°150) in order to obtain a 0.4 mg cm^{-2}Pt loading. The cathodic ink was prepared in a 5 ml high density polyethylene vial, mixing 200 mg of the commercial Pt (40 wt%)/C in

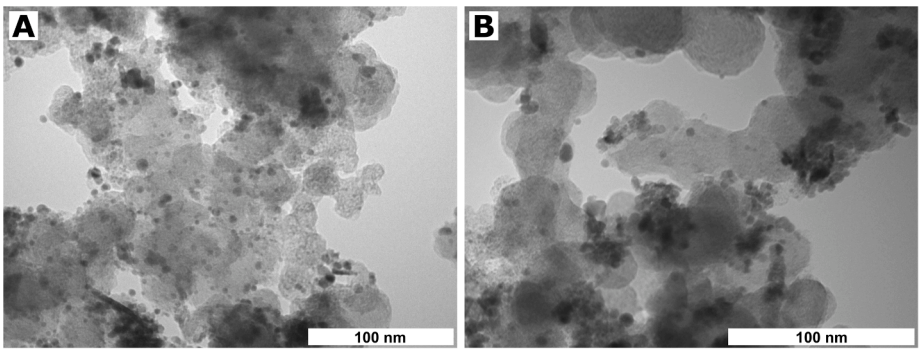

Fig. 2. TEM micrographs of Pd-CeO_2/C. Scale bar is 100 nm.

450 mg of distilled water, 790 mg of 1-propanol, and 1.56 g of the ionomer Nafion (5 wt% in 2-propanol). The mixture was suspended by ultrasound treatment. The anode catalyst ink was prepared by mixing the Pd-CeO_2/C catalyst (40 mg) with water (400 mg) and 40 mg of a 10 wt% PTFE aqueous suspension (10% PTFE final loading of the dried electrode). The resulting thick paste was spread evenly onto a 4 cm^2 nickel foam support (Heze Tianyu Technology Development Co, China) to obtain a Pd loading of ca. 1 mg cm^{-2}. The active electroreformer cell was purchased from Scribner-Associates (USA) (25 cm^2 fuel cell fixture). The MEA were fabricated by mechanically pressing the anode, the Pt/C cathode and the membrane within the cell hardware (6 Nm torque).

2.1.4. Electrolysis cell testing

The fuel solution used was 30 ml of a 2 M KOH and 2 M of alcohol or formate aqueous solution. Potassium formate, methanol, ethanol, 1,2-propandiol, ethylene glycol, glycerol or 1,4-butanediol purchased from Sigma-Aldrich-Merck were tested. The cell anode was fed recirculating the fuel in the anode compartment by means of a peristaltic pump with a 1 ml min^{-1} flow rate.

Voltage scans and galvanostatic curves were acquired using an ARBIN BT-2000 5A-4 channels potentiostat/galvanostat. Chronopotentiometry experiments were performed by applying a constant electrolysis current of 30 mA cm^{-2} until the cell voltage reached the value of 1.0 V.

The fuel solutions were recovered after each experiment and were quantitatively and qualitatively analyzed by $^{13}C\{^1H\}$ NMR spectroscopy and HPLC. NMR spectra were acquired with a with a Bruker Avance DRX 400 spectrometer. Chemical shifts (δ) are reported in ppm relative to TMS (^1H and ^{13}C NMR spectra). Deuterated solvents (Sigma-Aldrich) used for NMR measurements were dried with activated molecular sieves; 1,4-dioxane was used as internal standard for product quantification. A UFLC Shimadzu chromatograph equipped with refraction index detector (RID) was used; the column is a GRACE-Alltech OA-1000 organic acid (300 mm × 6.5 mm), thermostated at 65 °C. The eluent is 0.01 N H_2SO_4, and the eluent flow is 0.4 ml min^{-1}.

The hydrogen generated during the electroreforming was recorded by a Bronkhorst EL-FLOW mass flow meter model F-101C-002-AGD-11-V with a maximum H_2 flow rate of 3 ml min^{-1}.

3. Results and discussions

The Pd-CeO_2/C catalyst was synthesized following a well-established procedure [38] and the resulting catalyst morphology was characterized by TEM microscopy. Fig. 2 shows a TEM micrograph of the catalyst at low magnification (Fig. 2A) and high magnification (Fig. 2B). CeO_2 nanoparticle clusters are heterogeneously distributed over the carbon support. Pd NPs are mixed intimately with the CeO_2 clusters.

A comprehensive STEM-EDX and XAS analysis of this catalyst described in previous publications demonstrates a preferential Pd deposition in the support regions where ceria accumulates during the

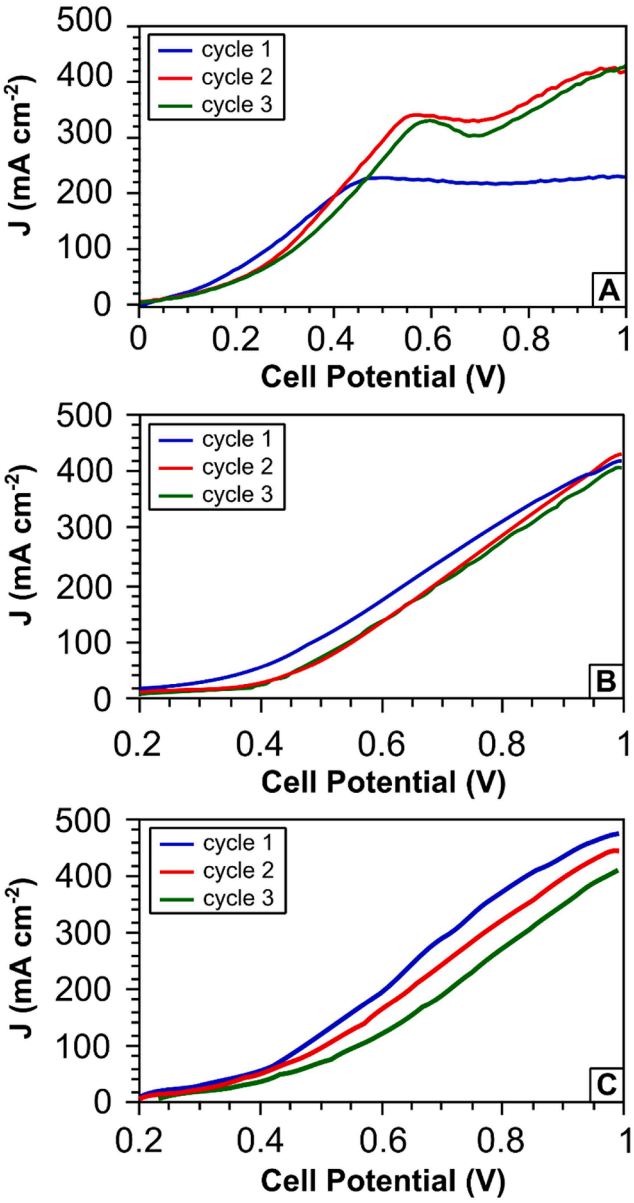

Fig. 3. Scan voltage curves of the electroreformer fed with an aqueous 2 M KOH and 2 M formate (A) or 2 M methanol (B) or 2 M ethanol (C) solutions; 10 mV s^{-1} scan rate. Each cell was subjected to three consecutive experiments: cycle 1 (blue curve), cycle 2 (red curve) and cycle 3 (green curve). A fresh fuel batch was used for any experiment.

Table 1
Catalytic data of electroreforming with Pd-CeO_2/C at the anode at 60 °C. 1,2-P = 1,2-propandiol, EG = ethylene glycol, Gly = glycerol, 1,4-B = 1,4-butanediol.

Entry	Fuel	Cycle	J_{max} @ 1 V (mA cm^{-2})	E_{onset} (V)	H_2 (mmol)	Energy Consumption (kWh $kg^{-1}H_2$)	Conversion (%)
1	$HCOO^-$	1	228	0.05	41	5.1	69
		2	414	0.10	50	6.1	83
		3	424	0.10	48	6.7	80
2	MeOH	1	422	0.36	88	15.6	84
		2	437	0.43	83	17.1	78
		3	415	0.43	85	17.6	80
3	EtOH	1	474	0.35	65	11.7	95
		2	448	0.35	70	14.3	95
		3	411	0.40	70	15.2	97
4	1,2-P	1	529	0.41	107	17.5	75
		2	424	0.39	110	17.6	79
		3	307	0.54	104	18.1	78
5	EG	1	249	0.41	91	16.3	70
		2	312	0.45	97	16.9	70
		3	446	0.44	99	17.4	72
6	Gly	1	196	0.48	89	15.2	49
		2	496	0.53	94	15.9	53
		3	425	0.55	94	15.7	55
7	1,4-B	1	495	0.25	99	12.8	64
		2	434	0.34	103	18.2	67
		3	255	0.58	105	21.4	70

synthesis. This architecture generates an intimate contact between ceria and palladium nanoparticles promoting the hydroxide ions spillover to Pd NPs and so improving the catalyst activity toward alcohol electro-oxidation reaction as previously reported in literature [32,36].

The Pd-CeO_2/C catalyst applied to a nickel foam with PTFE was assembled in the electroreforming cell. The device was equipped with a commercial Pt/C cathode spread onto a carbon cloth gas diffusion layer and the commercial Tokuyama A201 anion exchange membrane. Electroreforming experiments were performed at the cell temperature of 60 °C. Higher temperatures were not explored to avoid membrane damage. The cell activity was investigated by means of scan voltage experiments from 0 to 1.2 V. Fig. 3 shows the curves acquired for the electroreformers fed with aqueous 2 M KOH and 2 M $HCOO^-$ or MeOH or EtOH. The maximum current density of 424 mA cm^{-2} (Fig. 3A and table 1, entry 1), of 437 mA cm^{-2} (Fig. 3B and table 1, entry 2) and of 474 mA cm^{-2} (Fig. 3C and table 1, entry 3) was recorded respectively for formate, methanol and ethanol based feeding solution at a cell voltage of 1 V. All the tested electroreformers performance was stable over the

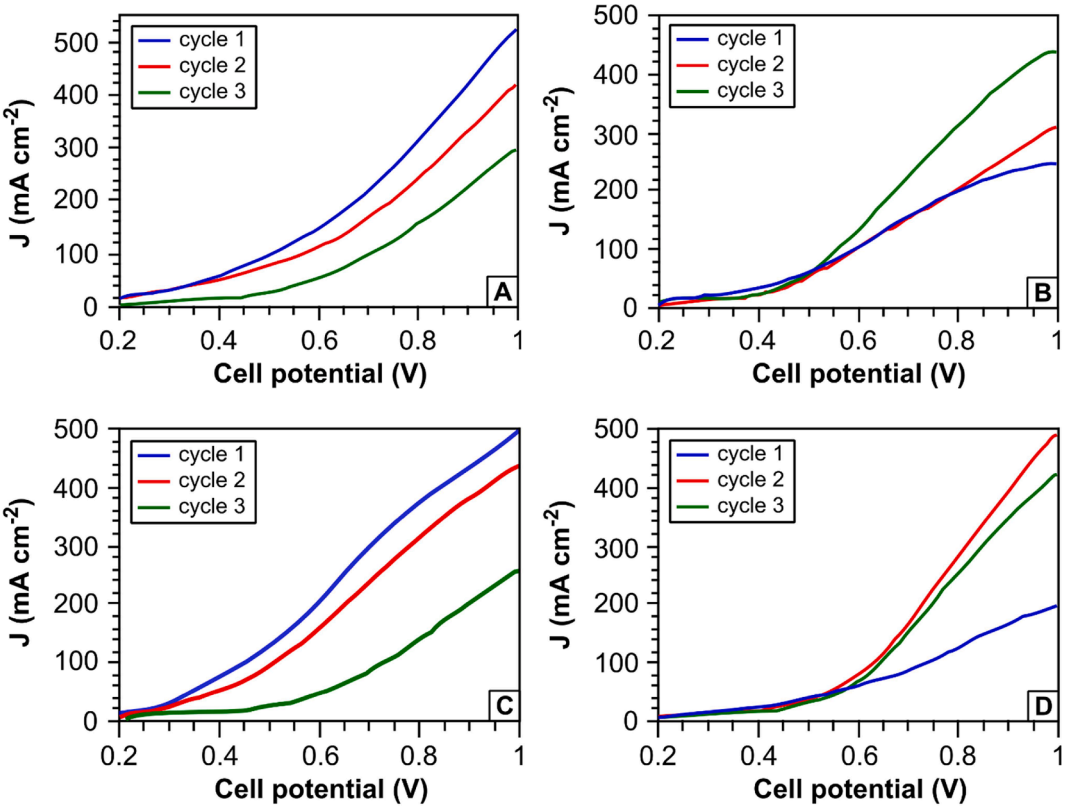

Fig. 4. Scan voltage characterization of the electroreformers fed with an aqueous 2 M KOH and 2 M 1,2-propandiol (A) or 2 M ethylene glycol (B) or 2 M 1,4-butandiol (C) or 2 M glycerol (D); 10 mV s^{-1} scan rate. Each cell was subjected to three consecutive experiments: cycle 1 (blue curve), cycle 2 (red curve) and cycle 3 (green curve). A fresh fuel batch was used for any experiment.

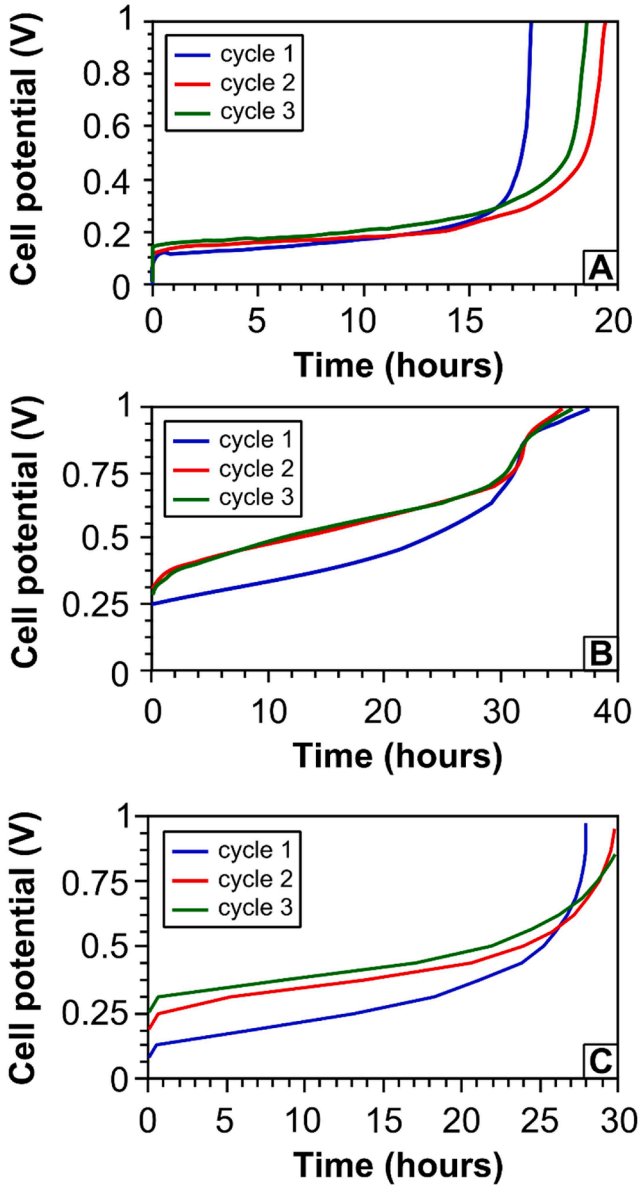

Fig. 5. Electroreforming of aqueous 2 M KOH 2 M formate (A) or 2 M methanol (B) or 2 M ethanol (C) at 30 mA cm^{-2} current load. Each cell was subjected to three consecutive experiments using a fresh fuel solution for every galvanostatic: cycle 1 (blue curve), cycle 2 (red curve) and cycle 3 (green curve).

three batch experiments indicating no loss in performance during electrocatalysis from batch to batch.

In the case of $HCOO^-$ fed cell, the first experiment shows the low Pd-CeO_2/C activity of 228 mA cm^{-2} @ 1 V for fuel oxidation. The maximum current density at 1 V then increases in the following tests, reaching the values of 414 and 424 mA cm^{-2} respectively in the second and in the third scan. Probably a catalyst stabilization occurs during the first scan, leading to a Pd-CeO_2/C reactivation. In fact, the reversible formation of poisoning palladium oxides onto the nanoparticles surface is a typical phenomenon of palladium-ceria catalysts due to the strong oxophilic CeO_2 behavior [38]. Scan voltages acquired for formate oxidation looks very different respect the other curves of the series. Formate oxidation onset potential is very low, c.a. 0.1 V (table 1, entry 1), while for MeOH and EtOH oxidation starts at c.a. 0.4 V (see table 1 entries 2 and 3). In general, formate and low aliphatic alcohols oxidation is enhanced by the OH^- ions spillover from ceria to Pd nanoparticles which leads to the formation of Pd(I)-OH_{ads} species at lower potential respect Pd/C catalyst [36]. Furthermore, formate oxidation is an easier reaction respect alcohols and polyols oxidation [27,30], so the ceria booster effect is more efficient and leads to a negligible overpotential reaction [22,30].

Despite the higher onset potential for MeOH and EtOH oxidation in the electroreformer, results are in line with the activity of ceria free cells reported in literature based on palladium or other precious metal anodes such as Rh/C [18,21].

The Pd-CeO_2/C based electroreformer is able to produce hydrogen and chemicals not only by the oxidation of small molecules such as EtOH, MeOH and $HCOO^-$, but also when it is fed with biomass-derived polyols, such as diols or glycerol. Fig. 4 summarizes the scan voltage curves acquired for 1,2-propandiol (Fig. 4A), ethylene glycol (Fig. 4B), 1,4-butanediol (Fig. 4C) and glycerol (Fig. 4D) fed cell (2 M KOH 2 M polyol aqueous fuel) and the electroreformer stability was again investigated by repeating three times each experiment with a batch of fresh fuel. The performance with the C_3 and C_4 diols dropped over the three consecutive batches during the three repeated experiments, for example for 1,2-propandiol the maximum current density recorded at 1 V drops from 529 mA cm^{-2} of the first cycle to 307 mA cm^{-2} of the third one (Fig. 4A and table 1, entry 4). Contemporaneously the onset potential increases from 0.41 V to 0.54 V. In a similar manner, the cell fed with 1,4-butanediol has a current drop from 495 to 255 mA cm^{-2} and an onset potential increase from 0.25 to 0.58 V (Fig. 5C and table 1, entry 7). By comparison, ethylene glycol ad glycerol fed electroreformers show a reverse trend, where the current density at 1 V increases from 249 to 446 mA cm^{-2} for ethylene glycol oxidation (Fig. 4B and table 1, entry 5) and from 196 to 425 mA cm^{-2} for glycerol oxidation (Fig. 4D and table 1, entry 6).

Constant current experiments with fixed volume fuel batches were undertaken to study the selectivity of oxidation for each alcohol as well as the stability over various batches. A constant current load of 120 mA (30 mA cm^{-2}) was applied to the cell and the voltage was recorded until the cut off potential of 1 V was reached. A flow meter was used to measure the hydrogen produced at the cathode electrode. Each galvanostatic experiment, named also potentiodynamic curve, was repeated three times for each cell, using a fresh fuel batch each time.

Fig. 5 shows the potentiodynamic curves for the 2 M KOH 2 M formate (Fig. 5A), 2 M methanol (Fig. 5B) and 2 M ethanol (Fig. 5C) solutions, while In Fig. 6 the experiments performed on the cells fed with polyols: 1,2-propandiol (Fig. 6A), ethylene glycol (Fig. 6B), 1,4-butanediol (Fig. 6C) and glycerol (Fig. 6D) are shown. The cell voltage recorded during electrolysis increases over time since the fuel is constantly converted into the products. Towards the end of each curve the potential rises sharply to 1 V. This occurs as the fuel concentration drops to a low level. The conversion efficiency was calculated from HPLC analysis of the fuel solution after each test. All the cells evolve c.a. 1.73 l min^{-1} m^{-2} of pure hydrogen with a Fradaic efficiency of c.a. 86–90%. The electrical energy consumed in each test is expressed in kWh $kg_{H_2}^{-1}$ and was evaluated for each experiment by integrating the instantaneous charging power over the experimental duration time. A summary of the data is shown in Table 1.

Formate is the substrate that requires the lowest energy input among the various alcohols studied, c.a 6 kWh $kg_{H_2}^{-1}$ (table 1, entry 1), due to the very low working potential, less than 0.25 V for c.a. 15 h of electrolysis (Fig. 5A). Methanol and ethanol fed electroreformers require a higher mean energy input, respectively 16.8 and 13.7 kWh $kg_{H_2}^{-1}$. The higher mean percentage of fuel converted to products among three experiments, 81% for MeOH and 95% for EtOH, reward the higher energy consumption of these cells. The low energy input and the higher conversion, coupled with a negligible toxicity, makes ethanol a more promising fuel than methanol

Diols and glycerol fed cells have a lower fuel conversion to products compared to ethanol and methanol fed devices (table 1, entries 4–7). Conversions span from 77.3% (mean value on three experiments) for 1,2-propandiol oxidation to 52.3% (mean value on three experiments) for the glycerol. In general, polyol oxidation promoted by palladium

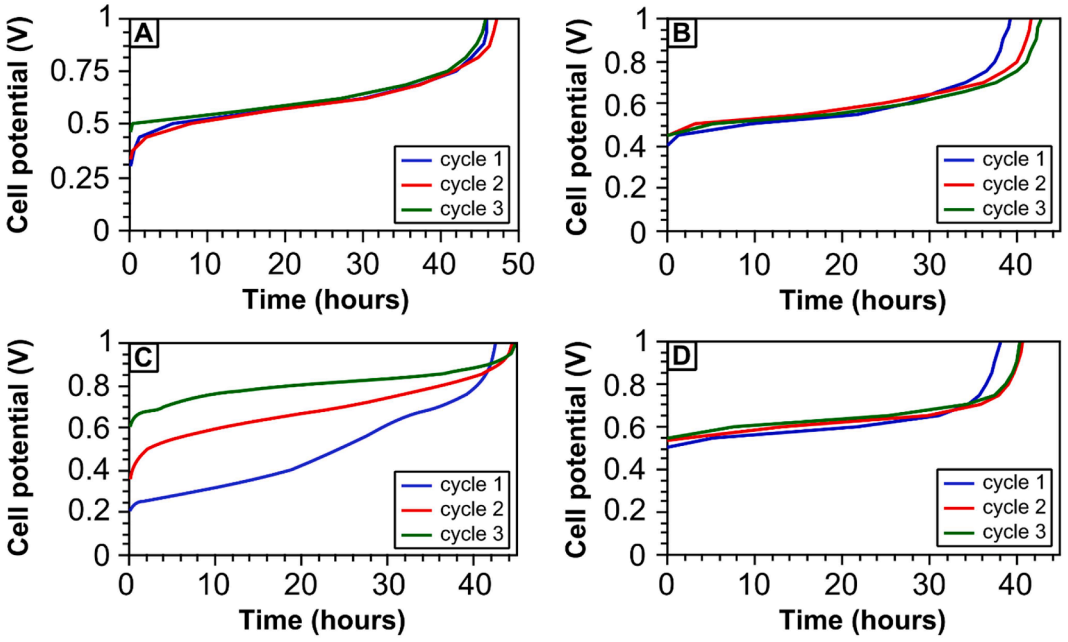

Fig. 6. Electroreforming of aqueous 2 M KOH 2 M 1,2-propandiol (A), 2 M ethylene glycol (B), 2 M 1,4-butanediol (C) and 2 M glycerol (D) at 30 mA cm^{-2} current load. Each cell was subjected to three consecutive experiments using a fresh fuel solution for every galvanostatic: cycle 1 (blue curve), cycle 2 (red curve) and cycle 3 (green curve).

based catalysts is less efficient than small alcohols oxidation, such as MeOH and EtOH [18]. This leads to a cell energy input increase, up to 17.7 kWh $kg_{H_2}^{-1}$ for the 1,2-propandiol fed reformer. For each cell, the three galvanostatics experiments are reproducible within the experimental variability, showing a high stability of the Pd-CeO_2/C anode for long term electrolysis at 60 °C and mild current loads (120 mA).

The main goal of the electroreforming technique is the very low energy input required for pure hydrogen production. The cell here studied is one of the most energy efficient electroreformer ever reported, with an electricity consumption spanning from 6 kWh $kg_{H_2}^{-1}$ for the formate fed cell to 17.7 kWh $kg_{H_2}^{-1}$ for 1,4-butanediol fed device. All these values are lower respect the 20 kWh $kg_{H_2}^{-1}$ energy consumption of the most performing electroreformes reported in literature [12,18].

From an overall energetic point of view, is the exploitation of renewable alcohols, such as bioethanol, convenient for hydrogen production by electroreforming with respect to water electrolysis?

Considering the overall ethanol electroreforming reaction (eq. (1)), the production of 1 kg of hydrogen (corresponding to 495 mol) requires the consumption of 11.4 kg of ethanol (247.5 mol) and 9.9 kg of sodium hydroxide (247.5 mol). NaOH was considered instead of KOH since no data on potassium hydroxide Life Cycle Assessment (LCA) are reported in literature.

$$CH_3CH_2OH + OH^- \rightarrow CH_3COO^- + 2H_2 \quad (1)$$

Sodium hydroxide production has an energy cost of 0.97 kWh kg_{NaOH}^{-1} [39] and one mole of alkali is consumed for producing one mole of dihydrogen (eq.1). So to evaluate the electroreformer overall energy consumption, 9.7 kWh $kg_{H_2}^{-1}$ per kilogram of produced hydrogen must be added to the electric energy input of the cell. The ethanol fed reformer here reported has a mean electricity consumption of 13.7 kWh $kg_{H_2}^{-1}$ (average value calculated over three cycles). In contrast, the best PEM water electrolyzers require c.a. 47 kWh $kg_{H_2}^{-1}$ of electricity to split water into hydrogen and oxygen, so ethanol electroreforming will gain a net energy saving for H_2 production only if the fuel (alcohol) energy cost is lower than 23.6 kWh $kg_{H_2}^{-1}$. This will be achieved only if the energy spent to produce the 1 kg of EtOH used in the electroreformer is less than 2.1 kWh kg_{EtOH}^{-1}. Bioethanol net energy cost is usually expressed in terms of the EROEI, namely, the ratio between the output energy of ethanol and the energy input required for its production. Ethanol obtained from first generation biomasses, such as corn, have an EROEI lower than 1, so more energy is spent for producing this fuel, compared to the energy contained in it [40,41]. Only a bioethanol EROEI larger than 5.1 will lead to a net energy saving in hydrogen production with respect to current water electrolysis technology. In conclusion, H_2 production by the electroreforming of bioethanol will be energetically convenient depending on the source of the alcohol, for example, by using sugarcane, which is commonly reported to have an EROEI of 8, and by using cellulose, which has an EROEI potentially up to 35, but not by using corn which have an EROEI lower than 1 [42–45].

Table 2
Fuel exhausts analysis by HPLC and ^{13}C NMR. 1,2-P = 1,2-propandiol, EG = ethylene glycol, Gly = glycerol, 1,4-B = 1,4-butanediol.

Entry	Fuel	Selectivity (%)
1	$HCOO^-$	Carbonate (100)
2	MeOH	Carbonate (95)
		Formate (5)
3	EtOH	Acetate (100)
4	1,2-P	Lactate (84)
		Acetate (7)
		Carbonate (9)
5	EG	Glycolate (81)
		Formate (13)
		Oxalate (4)
		Acetate (1)
		Carbonate (1)
6	Gly	Glycerate (48)
		Tartronate (28)
		Glycolate (4)
		Oxalate (2)
		Carbonate (19)
7	1,4-B	4-hydroxybutanate (58)
		Succinate (42)

The composition of the fuel solution after each test was quantitatively and qualitatively characterized using HPLC analysis and $^{13}C\{^1H\}$ NMR spectroscopy. Table 2 summarizes the oxidation product distribution and Fig. 7 shows the ^{13}C NMR spectra of the solutions recovered after the first cycle of each galvanostatic experiment. For formate the

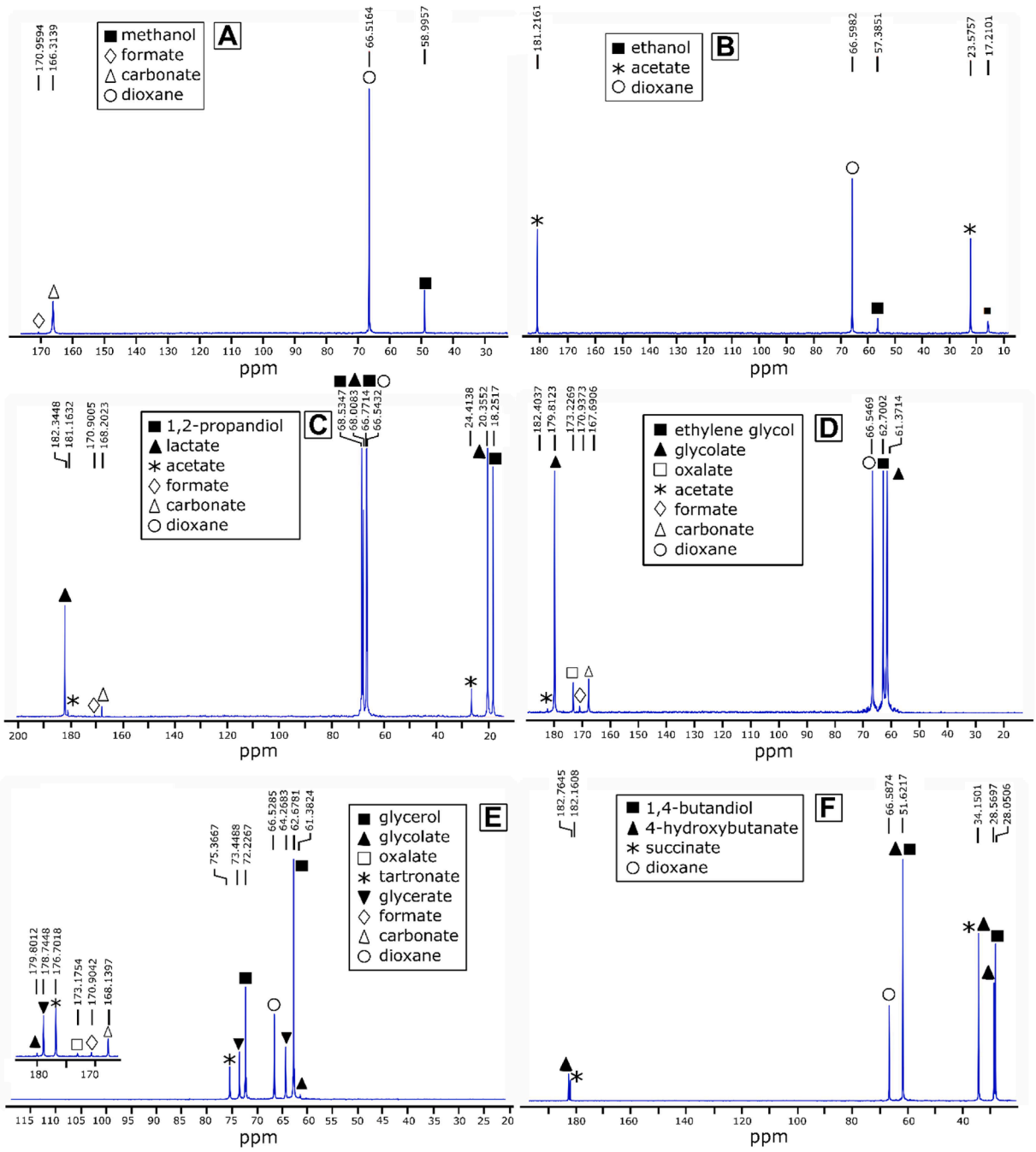

Fig. 7. ^{13}C NMR spectra of fuel exhaust solutions. (A) methanol, (B) ethanol, (C) 1,2-propandiol, (D) ethylene glycol, (E) glycerol and (F) 1,4-butanediol spent fuels.

spectra are not reported since carbonate is the only possible reaction product (100% selectivity, see table 2 entry 1), obtained following a $2e^-$ oxidative pathway. Methanol oxidation leads to 95% of carbonate through a $4e^-$ electrochemical process and only 5% of formate, obtained through a $2e^-$ pathway (Fig. 7A and table 2, entry 2). In contrast, for EtOH and the other polyols studied the oxidation reaction does not proceed to CO_3^{2-} but follows generally a four electron pathway leading to the formation of monocarboxylic compounds as principal products. This is a well-known feature of Pd and Pt based electrocatalysts when alcohol oxidation happens in strong alkaline media [5]. So in the case of ethanol, the only product obtained is acetate (100% selectivity), as described in Fig. 7B and table 2, entry 3. The main oxidation product of 1,2-propandiol is lactate, with 84% selectivity. The minor products acetate (7%) and carbonate (9%) are also present (Fig. 7C and table 2, entry 4) [29]. In a similar manner, the cell fed with ethylene glycol yields 81% of glycolate together with 13% of formate and 1% of acetate and carbonate (Fig. 7D and table 2, entry 5). Glycerol oxidation results in a mixture of products including glycerate (48%), tartronate (28%) and minor products, obtained from C—C chemical bond scission, such as oxalate, glycolate, formate and carbonate. No trace of the secondary alcohol oxidation products of glycerol such as dihydroxyacetone, hydroxypiruvate, or mesoxalate is observed (Fig. 7E and table 2, entry 6).

1,4-butanediol oxidation, leads to the formation a mixture of 58% of 4-hydroxybutanate and 42% of succinate (Fig. 7F and table 2, entry 7). The selectivity of polyol electrooxidation to the mono carboxylate is lower with increasing the aliphatic chain length because the oxidation of the residual alcohol groups in the obtained monocarboxylic product also occurs. A longer aliphatic chain will reduce the steric and electronic effects which may hinder oxidation of the monocarboxylic compound

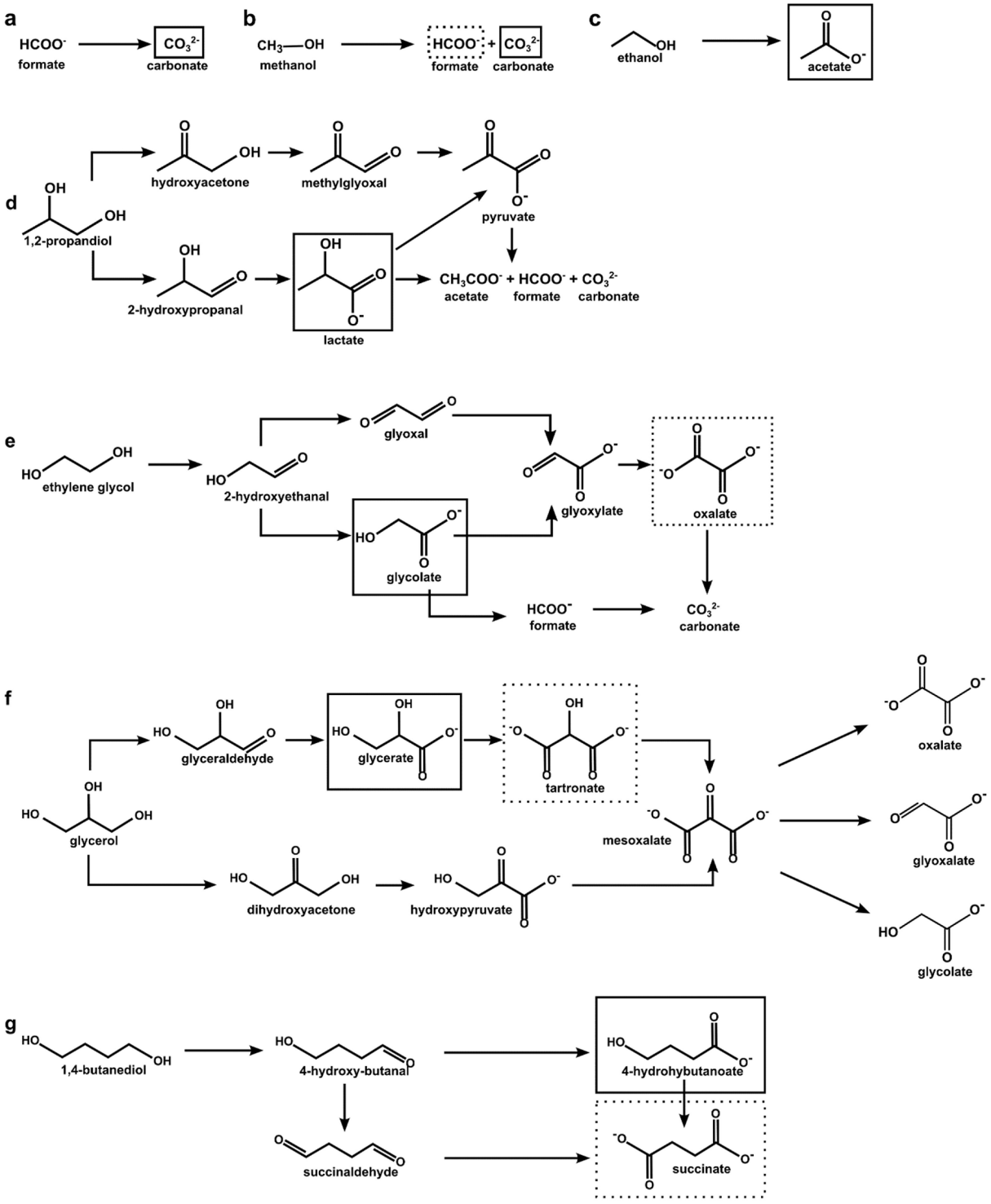

Scheme 1. A simplified oxidation mechanism of: (a) formate, (b) methanol, (c) ethanol; (d) 1,2-propandiol; (e) ethylene glycol; (f) glycerol and (g) 1,4-butanediol. Main products are evidenced in solid boxes, secondary products in dashed boxes.

[19]. So, in the case of ethylene glycol, a small molecule, the oxidation of glycolate is not favored and only a small amount of 4% of oxalate was obtained. In contrast, 1,4-butanediol oxidation leads to the formation of 58% of the monocarboxylate (4-hydroxybutanate) and 42% of the dicarboxylic compound (succinate). In a similar manner, regarding glycerol oxidation, the intermediate glycerate is readily oxidized and yields 28% of tartronate.

The oxidation mechanisms of 1,2-propandiol, ethylene glycol, glycerol and 1,4 butanediol promoted by Pd based catalysts has been thoroughly described in the literature [46–48] and are summarized in scheme 1 (reactions **d**, **e**, **f** and **g**). Solid boxes emphasize the primary products, while dashed boxes underline the minor products obtained from monocarboxylate oxidation to dicarboxylic compounds. The main products of reactions **c**-**g** where obtained oxidizing the alcohol to the corresponding aldehyde and two electrons. Such a reaction is considered the overall reaction rate determining step. The aldehyde is then quickly oxidized to the corresponding carboxylic compound and two electrons are released to the anode. So the overall reaction involves four electrons

[22]. In a similar manner, the main products are further oxidized to dicarboxylic products, since the oxidation involve the residual alcoholic group in the molecule.

The electrochemical reforming of alcohols in both acid and alkaline media has been extensively studied for a range of catalyst types [49]. In terms of reduced energy cost, Pd-CeO_2/C outperforms most catalyst types aside from Rh/C [21], while the 97% conversion efficiency of ethanol by Pd-CeO_2/C is the highest observed so far in electroreforming of alcohols.

4. Conclusions

This paper describes the performance of an electrochemical reformer using Pd-CeO_2/C as anode catalyst operating at 60 °C and fed with an alkaline solution of various alcohols. The fuels studied were: formate, MeOH, EtOH, 1,2-propandiol, ethylene glycol, glycerol and 1,4-butanediol. The results highlight the excellent and stable activity of Pd-CeO_2/C. The amount of electrical energy required for H_2 production for all alcohols is in the range of 6.0 – 17.7 kWh $kg_{H_2}^{-1}$. In particular, 13.7 kWh $kg_{H_2}^{-1}$ from EtOH results in an electrical energy saving of 33.3 kWh $kg_{H_2}^{-1}$ as compared with that reported by the DOE for PEM electrolyzer. Formate is also a very promising fuel since its electroreforming process to hydrogen and carbonate requires only 6 kWh $kg_{H_2}^{-1}$. The other aspect studied was the selectivity of alcohol oxidation in batch experiments. The electroreformer here presented was selective for MeOH oxidation to carbonate (95%), EtOH to acetate (100%), 1,2-propandiol oxidation to lactate (84%), ethylene glycol to glycolate (81%). The other polyols (ethylene glycol and 1,4-butanediol) were oxidized to more complex mixtures of partial oxidation products. For the first time we have demonstrated how an electrochemical reformer can operate with seven alcohol fuels. It can be envisaged that this technology can accommodate high variability in bioalcohol availability and market fluctuation as well as geographical and seasonal variability. The Pd-CeO_2/C catalyst exhibits superior conversion efficiencies over the whole range of alcohols studied. Combined with high stability and selectivity for valuable chemicals distinguishes this catalyst as ideal candidate for the industrialization of electrochemical reforming in the future.

CRediT authorship contribution statement

Marco Bellini: Investigation, Formal analysis. **Maria V. Pagliaro:** Investigation, Visualization. **Andrea Marchionni:** Investigation, Visualization. **Jonathan Filippi:** Writing - review & editing, Visualization. **Hamish A. Miller:** Investigation, Formal analysis. **Manuela Bevilacqua:** Investigation. **Alessandro Lavacchi:** Investigation, Validation, Data curation. **Werner Oberhauser:** Investigation. **Jafar Mahmoudian:** Investigation. **Massimo Innocenti:** Conceptualization. **Paolo Fornasiero:** Conceptualization, Writing - original draft, Supervision. **Francesco Vizza:** Conceptualization, Supervision, Project administration, Funding acquisition.

Declaration of Competing Interest

The authors declare that they have no known competing financial interests or personal relationships that could have appeared to influence the work reported in this paper.

Acknowledgements

The authors would like to thank the Italian ministry MIUR through the PRIN 2017 “Novel Multilayered and Micro-Machined Electrode Nano-Architectures for Electrocatalytic Applications (Fuel Cells and Electrolyzers).

Bibliography

[1] R.L. Orbach, Energy Production: A Global Perspective, 2012.
[2] D.J. Murphy, C.A.S. Hall, Ann. N. Y. Acad. Sci. 1219 (2011) 52–72.
[3] T.K. Ghosh, M.A. Prelas, Energy Resources and Systems. Volume 1 - Fundamentals and Non-Renewable Resources, 2009.
[4] S. van Renssen, Nat. Clim. Chang. 10 (2020) 799–801.
[5] A. Lavacchi, H. Miller, F. Vizza, Nanotechnol. Electrocatal. Energy (2013).
[6] P. Nikolaidis, A. Poullikkas, Renew. Sustain. Energy Rev. 67 (2017) 597–611.
[7] L. Barreto, A. Makihira, K. Riahi, Int. J. Hydrogen Energy 28 (2003) 267–284.
[8] S. Sharma, S.K. Ghoshal, Renew. Sustain. Energy Rev. 43 (2015) 1151–1158.
[9] J.A. Turner, Science 305 (2004) 972–974.
[10] S. Marini, P. Salvi, P. Nelli, R. Pesenti, M. Villa, M. Berrettoni, G. Zangari, Y. Kiros, Electrochim. Acta 82 (2012) 384–391.
[11] M. Carmo, D.L. Fritz, J. Mergel, D. Stolten, Int. J. Hydrogen Energy 38 (2013) 4901–4934.
[12] Y.X. Chen, A. Lavacchi, H.A. Miller, M. Bevilacqua, J. Filippi, M. Innocenti, A. Marchionni, W. Oberhauser, L. Wang, F. Vizza, Nat. Commun. 5 (2014) 4036.
[13] Z. Hu, M. Wu, Z. Wei, S. Song, P.K. Shen, J. Power Sources 166 (2007) 458–461.
[14] T. Take, K. Tsurutani, M. Umeda, J. Power Sources 164 (2007) 9–16.
[15] V. Bambagioni, M. Bevilacqua, C. Bianchini, J. Filippi, A. Lavacchi, A. Marchionni, F. Vizza, P.K. Shen, ChemSusChem 3 (2010) 851–855.
[16] F. Vitse, M. Cooper, G.G. Botte, J. Power Sources 142 (2005) 18–26.
[17] M. Cooper, G.G. Botte, J. Electrochem. Soc. 153 (2006) A1894.
[18] H.A. Miller, M. Bellini, F. Vizza, C. Hasenöhrl, R.D. Tilley, Catal, Sci. Technol. 44 (2016) 7540–7590.
[19] M. Bellini, J. Filippi, H.A. Miller, W. Oberhauser, F. Vizza, Q. He, H. Grützmacher, ChemCatChem 9 (2017) 746–750.
[20] J. Mahmoudian, M. Bellini, M.V. Pagliaro, W. Oberhauser, M. Innocenti, F. Vizza, H.A. Miller, ACS Sustain. Chem. Eng. (2017).
[21] M.V. Pagliaro, M. Bellini, M. Bevilacqua, J. Filippi, M.G. Folliero, A. Marchionni, H.A. Miller, W. Oberhauser, S. Caporali, M. Innocenti, F. Vizza, RSC Adv. 7 (2017) 13971–13978.
[22] C. Bianchini, P.K. Shen, Chem. Rev. 109 (2009) 4183–4206.
[23] S. Zinoviev, F. Müller-Langer, P. Das, N. Bertero, P. Fornasiero, M. Kaltschmitt, G. Centi, S. Miertus, ChemSusChem 3 (2010) 1106–1133.
[24] N.S. Bentsen, C. Felby, Biotechnol. Biofuels 5 (2012) 1–10.
[25] E. Kirtay, Energy Convers. Manag. 52 (2011) 1778–1789.
[26] C.B. Field, J.E. Campbell, D.B. Lobell, Trends Ecol. Evol. 23 (2008) 65–72.
[27] H. Miller, J. Ruggeri, A. Marchionni, M. Bellini, M. Pagliaro, C. Bartoli, A. Pucci, E. Passaglia, F. Vizza, Energies 11 (2018) 369.
[28] T. Vo, K. Purohit, C. Nguyen, B. Biggs, S. Mayoral, J.L. Haan, ChemSusChem 8 (2015) 3853–3858.
[29] M. Bellini, M. Bevilacqua, M. Innocenti, A. Lavacchi, H.A. Miller, J. Filippi, A. Marchionni, W. Oberhauser, L. Wang, F. Vizza, J. Electrochem. Soc. 161 (2014) D3032–D3043.
[30] L.Q. Wang, M. Bellini, J. Filippi, M. Folliero, A. Lavacchi, M. Innocenti, A. Marchionni, H.A. Miller, F. Vizza, Appl. Energy 175 (2016) 479–487.
[31] L. Wang, A. Lavacchi, M. Bevilacqua, M. Bellini, P. Fornasiero, J. Filippi, M. Innocenti, A. Marchionni, H.A. Miller, F. Vizza, ChemCatChem 7 (2015) 2214–2221.
[32] A. Lenarda, M. Bellini, A. Marchionni, H.A. Miller, T. Montini, M. Melchionna, F. Vizza, M. Prato, P. Fornasiero, Inorganica Chim. Acta 470 (2018) 213–220.
[33] M. Melchionna, M. Bevilacqua, P. Fornasiero, Mater. Today Adv. 6 (2020) 100050–100061.
[34] A. Beltram, M. Melchionna, T. Montini, L. Nasi, R.J. Gorte, M. Prato, P. Fornasiero, Catal. Today 253 (2015) 142–148.
[35] G. Valenti, M. Melchionna, T. Montini, A. Boni, L. Nasi, E. Fonda, A. Criado, A. Zitolo, S. Voci, G. Bertoni, M. Bonchio, P. Fornasiero, F. Paolucci, M. Prato, A.C. S. Appl, Energy Mater. 3 (2020) 8509–8518.
[36] V. Bambagioni, C. Bianchini, Y. Chen, J. Filippi, P. Fornasiero, M. Innocenti, A. Lavacchi, A. Marchionni, W. Oberhauser, F. Vizza, ChemSusChem 5 (2012) 1266–1273.
[37] S.D. Minteer, Biochemical Production of Other Bioalcohols: Biomethanol, Biopropanol, Bioglycerol, and Bioethylene Glycol, Elsevier, 2011.
[38] H.A. Miller, A. Lavacchi, F. Vizza, M. Marelli, F. Di Benedetto, F. D'Acapito, Y. Paska, M. Page, D.R. Dekel, Angew. Chemie Int. Ed. 55 (2016) 6004–6007.
[39] L. Thannimalay, S. Yusoff, Z.Z. Norliyana, Aust. J. Basic Appl. Sci. 7 (2013) 421–431.
[40] J.E.A. Seabra, I.C. Macedo, M.R.L.V. Leal, Greenhouse Gases Emissions Related to Sugarcane Ethanol, Editora Edgard Blücher (2014).
[41] D. Pimentel, T.W. Patzek, Nat. Resour. Res. 14 (2005) 65–76.
[42] P.W. Gallagher, W.C. Yee, H.S. Baumes, 2015 Energy Balance for the Corn-Ethanol Industry, 2016.
[43] C.F. Ruviaro, M. Gianezini, F.S. Brandão, C.A. Winck, H. Dewes, J. Clean. Prod. 28 (2012) 9–24.
[44] J.E.A. Seabra, I.C. Macedo, H.L. Chum, C.E. Faroni, C.A. Sarto, Biofuels Bioprod. Biorefining 5 (2011) 519–532.
[45] C.A.S. Hall, B.E. Dale, D. Pimentel, Sustainability 3 (2011) 2413–2432.
[46] M. Simões, S. Baranton, C. Coutanceau, Appl. Catal. B Environ. 93 (2010) 354–362.
[47] Y. Kwon, K.J.P. Schouten, M.T.M. Koper, ChemCatChem 3 (2011) 1176–1185.
[48] A. Marchionni, M. Bevilacqua, C. Bianchini, Y.X. Chen, J. Filippi, P. Fornasiero, A. Lavacchi, H. Miller, L. Wang, F. Vizza, ChemSusChem 6 (2013) 518–528.
[49] H.A. Miller, A. Lavacchi, F. Vizza, Curr. Opin. Electrochem. 21 (2020) 140–145.